Direct determination of molecular orbital symmetry of H_2S using polarized x-ray emission

R. Mayer, D. W. Lindle, S. H. Southworth, and P. L. Cowan
National Institute of Standards and Technology, Gaithersburg, Maryland 20899
(Received 22 August 1990)

X-ray emission from the molecule H_2S is strongly polarized following excitation of a sulfur K-shell electron to an unoccupied subthreshold molecular orbital with a polarized x-ray beam. Changes in the polarization of the emission spectrum are observed as the incident beam's energy is swept across the subthreshold absorption resonance. The previously unresolved absorption resonance is shown experimentally to be primarily associated with a molecular orbital of b_2 symmetry, but with a high-excitation-energy component due to an orbital with a_1 symmetry. Satellite emission intensity is shown to depend on the primary photon energy and is therefore associated with multivacancy effects and not with contamination, as previously suggested.

INTRODUCTION

The geometrical and electronic structure of atoms and molecules has long been studied through the interpretation of x-ray absorption spectra (XAS) and x-ray emission spectra (XES).[1] The identification of the molecular symmetries[1,2] associated with features in XAS and XES has been achieved indirectly by comparing experimentally observed energies and relative intensities with molecular-orbital (MO) calculations. Although this procedure is often successful, a direct method for determining symmetries of MO's would be preferable, especially for disputed structures. In the case of x-ray absorption or emission, important identifying features are sometimes obscured due to lifetime broadening or are otherwise unresolved, thereby making an interpretation of the spectra problematic. In addition, XES excited by electrons or x rays with broad bandpass or high-energy x-ray sources often exhibit multivacancy emission satellites which complicate the interpretation.[1] Recently, selective excitation of XES by tunable monochromatic x rays has been used to eliminate[3] and study[4] multivacancy emission satellites.

Direct experimental determination of the symmetries associated with x-ray features in small molecules is based on a predicted[5] and recently observed phenomenon.[6] By tuning a monoenergetic polarized x-ray beam so as to promote a K-shell electron to an unoccupied valence orbital, molecules aligned with respect to the incident beam polarization can be selected from a random ensemble of free molecules.[6] The associated x-ray emission process occurs quickly ($\tau \sim 10^{-14}$ sec) relative to molecular rotations ($\sim 10^{-12}$ sec) and thus before any significant dealignment of the molecules. If the core hole is filled by an electron from a valence MO, it can result in polarization of a fluorescence component.[7,8]

Previously,[6] polarized x-ray emission was used to study CH_3Cl, belonging to the symmetry group C_{3v}, and whose major subthreshold absorption resonance is attributed to only a single MO. In contrast, the molecule H_2S, which is studied here, belongs to the symmetry group C_{2v} and has a subthreshold absorption resonance (see Ref. 9 and references cited therein) which is predicted to be composed of excitations to $3b_2$ and $6a_1$ orbitals.[10,11] Both theories[10,11] propose small absolute energy differences (approximately 1 eV) in the two unoccupied MO's, but they differ in the predicted order of their energies. The symmetry determination of the XAS feature is achieved by examining the polarization of selectively excited XES. Each K-V ($K\beta$) x-ray peak, where K-V refers to emission due to a valence electron filling the S K hole, in the emission spectrum is due to a single MO. The polarization of the K-V emission was found to vary as the primary photon energy was swept across the subthreshold absorption resonance. The variation of the polarization of the K-V emission is attributed to contributions from unresolved excitation to the two predicted absorption resonances having different symmetries. This is the first study to determine the S K-shell absorption symmetry in H_2S and it demonstrates an interesting application of polarized-emission measurements. In addition, selective excitation at energies above the ionization threshold permitted the study of the formation of an emission satellite and resolved a disagreement[12,13] over its origin. The observation of the satellite onset as the incident x-ray energy is raised above threshold suggests that the satellite originates initially from simultaneous K-hole formation and promotion of a valence electron to a low-lying unoccupied orbital, and at higher energies the satellite also derives intensity from double ionization. This observation supports the suggestion that the satellite originates from multiple-excitation processes[13] rather than contamination of the gas cell.[12] Emission due to the more tightly bound occupied $4a_1$ inner-valence orbital was not observable, despite a predicted[14] relative intensity of 0.03 with respect to the more intense K-V features and a detection limit of 0.01.

EXPERIMENT

To observe the polarization of x-ray fluorescence, an intense (10^{11}–10^{12} photons/sec), tunable beam of highly

Work of the U. S. Government
Not subject to U. S. copyright

monenergetic x rays from beamline X-24A (Ref. 15) at the National Synchrotron Light Source is used to excite or ionize the sample gas. A large-aperture monochromator[16] selects the desired incident x-ray energy and a toroidal mirror[17] focuses the beam to a small diameter (approximately 1 mm) at the target gas cell (approximately 100 Torr H_2S). The incident beam is linearly polarized due to the intrinsic polarization of the synchrotron radiation originating from the plane of the storage-ring orbit and due to the conservation and enhancement of the polarization by the optical components (monochromator, mirrors, slits) within the beamline. A secondary x-ray emission spectrometer[18] records the entire K-V energy spectrum by dispersing the radiation with a curved InSb(111) crystal and detecting the radiation with a position sensitive detector[19] with a combined 1.1-eV instrumental resolution. In addition, polarization sensitivity is achieved through Bragg diffraction of the sulfur K-V radiation with energy approximately 2.5 keV, at 42° incident angle on the InSb(111) crystal. With these scattering conditions, the transmission of radiation polarized within the dispersion plane of the spectrometer is less than 2% of that polarized perpendicular to this plane. The secondary spectrometer is positioned to detect K-V fluorescence emitted at 90° with respect to both the polarization direction and the propagation direction of the incident x rays. The XES dependence on polarization is measured by rotating the secondary spectrometer about the emission axis so as to transmit radiation polarized parallel or perpendicular with respect to the primary x-ray polarization. The gas cell is sealed with Mylar (not beryllium) windows to reduce the interaction of H_2S with the window. The attenuation of x rays through the Mylar is similar to that through the beryllium windows. Nevertheless, evidence for contamination of the windows by sulfur compounds appeared after 48 h of exposure to a flux of $10^{11}-10^{12}$ $sec^{-1}mm^{-2}$ of 2.5-keV photons and required periodic replacement of the windows. In addition, the x-ray catalyzed reaction resulted in a weakening of the structural strength of the Mylar. A third Mylar window was used to pass the x-ray fluorescence. Due to the low flux of photons hitting the emission window, the latter remained intact for the duration of the experiment. With the right-angle excitation and detection geometry, no sulfur XES originating from the contaminated windows was detected when the gas cell was evacuated. To determine absorption within the gas cell, the photocurrent from carbon foils placed before and after the sample was measured.

RESULTS: SYMMETRY OF SUBTHRESHOLD ABSORPTION RESONANCE AND POLARIZED FLUORESCENCE

Figure 1 shows the S K-V emission spectra from H_2S for photons polarized parallel ($\theta=0°$) and perpendicular ($\theta=90°$) to the incident-beam polarization direction and with the incident-beam energy tuned to the peak of the major subthreshold resonance. The solid lines are generated from fitting the data with a sum of four Voigt peaks (Lorentzian peaks convolved with an instrumental Gaussian function). The main features in the XES for H_2S, unlike the resonance in XAS, are well understood. The peaks labeled A, B, and C (using the convention of Mazalov *et al.*[12] and LaVilla[13]) correspond to $2b_1 \rightarrow 1a_1$, $5a_1 \rightarrow 1a_1$, and $2b_2 \rightarrow 1a_1$ transitions, respectively, where $1a_1$ is the S K-shell MO. The valence MO's of H_2S also have been studied using electron spectroscopy.[20–22] The MO's are derived from sulfur $3p$ and hydrogen $1s$ atomic orbitals, $5a_1$, S $3p_z$ and H(1)$1s$ + H(2) $1s$; $2b_2$, S $3p_y$ and H(1) $1s$ + H(2) $1s$; and the nonbonding orbital $2b_1$, S $3p_x$. It should be noted that for the case of subthreshold resonant excitation, the description of the K-V transitions given above should be modified to include the presence of a spectator electron. The highest energy peak in Fig. 1 is due to the elastically scattered beam and is suppressed as expected when the polarizer is tuned to $\theta=90°$ with respect to the incident beam polarization. (The elastically scattered beam experiences some resonance depolarization and self-absorption and so the ultimate polarization sensitivity and energy resolving

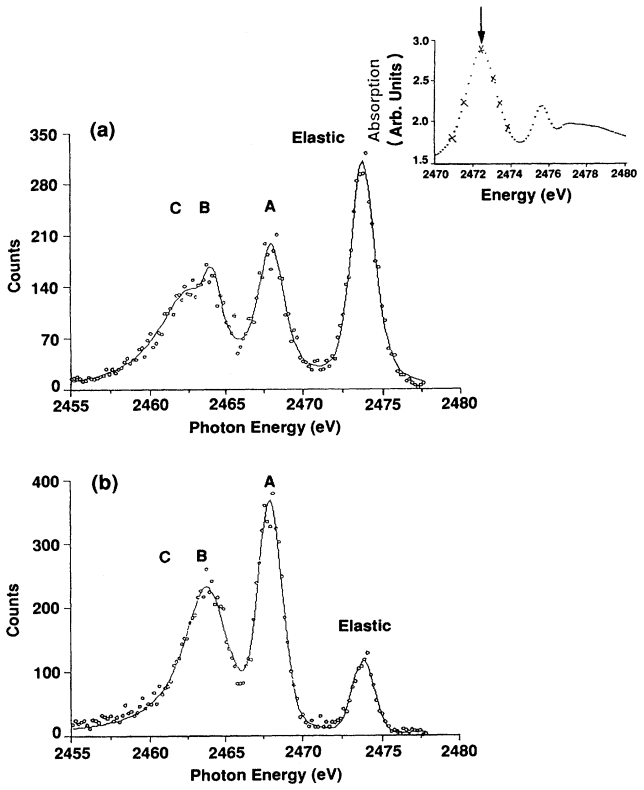

FIG. 1. Sulfur K-V ($K\beta$) emission spectra from H_2S with the polarimeter set to detect (a) parallel ($\theta=0°$) or (b) perpendicular ($\theta=90°$) polarized x rays with respect to the incident-beam polarization. The solid curves are fits using four Voigt peaks. Emission peak A denotes $2b_1 \rightarrow 1a_1$, B indicates $5a_1 \rightarrow 1a_1$, and C denotes $2b_2 \rightarrow 1a_1$. The inset shows absorption near threshold. The arrow denotes incident-beam energy, on resonance. The extra markings on the absorption resonance denote the excitation energies used to measure the K-V polarizations in Fig. 3.

power of the secondary spectrometer are not apparent.) The energy scale was calibrated using the energy values of LaVilla's[13] emission spectrum. It should be evident that the relative intensities of the emission peaks labeled C (A and B) are suppressed (enhanced) when the spectrometer is aligned to detect $\theta=90°$ polarization relative to the $\theta=0°$ polarization. This qualitative observation suggests that the peaks have strong polarizations of opposite sign.

The polarized emission spectra shown in Fig. 2 are generated using primary photons with slightly higher energy (approximately 1 eV) than those used in Fig. 1. Although both spectra suggest a strong suppression of the C ($2b_2$) peak for $\theta=90°$, a comparison of the two emission spectra reveals subtle differences. For example, as the primary beam energy is raised, the intensity of the B ($5a_1\rightarrow 1a_1$) peak increases relative to the A ($2b_1\rightarrow 1a_1$) peak in the $\theta=0°$ spectra in Figs. 1 and 2. Qualitatively, this observation suggests a variation in the polarizations of the emission peaks as the excitation energy is raised slightly above the absorption resonance maximum.

To further examine these observations, quantitative polarization values were generated from the experimental data. Determination of the polarization $P=(I_{0°}-I_{90°})/(I_{0°}+I_{90°})$ of the individual components in the emission spectra requires the measurement of the integrated intensities $I_{0°}$ and $I_{90°}$ taken at polarization angles $\theta=0°$ and 90°, respectively, for each of the emission peaks A, B, and C. The procedure for experimentally determining the polarizations has been discussed.[23] The relative contributions $m_{0°}(R)$ and $m_{90°}(R)$ of each of the emission peaks A, B, and C to the total emission spectra [$S_{0°}(R)$ and $S_{90°}(R)$, respectively] for primary photon energies near resonance R and taken at $\theta=0°$ and 90° are determined from numerical fits using Voigt functions. The relative emission peak fractions are corrected for differences in total number of primary photons Q during the emission measurement and normalized to unpolarized spectra generated by ionization well above threshold (AT) as follows:

$$\frac{I_{0°}}{I_{90°}}=\frac{m_{0°}(R)}{m_{90°}(R)}\frac{S_{0°}(R)}{S_{90°}(R)}\frac{Q_{90°}(R)}{Q_{0°}(R)} \times\frac{m_{90°}(\mathrm{AT})}{m_{0°}(\mathrm{AT})}\frac{S_{90°}(\mathrm{AT})}{S_{0°}(\mathrm{AT})}\frac{Q_{0°}(\mathrm{AT})}{Q_{90°}(\mathrm{AT})} . \quad (1)$$

Taking ratios as shown in Eq. (1) eliminates the need to measure the secondary spectrometer efficiency, which may vary with detector angle θ. The normalization to the total emission intensity S, using spectra recorded over fairly short time periods, accounts for effects due to window contamination and small primary beam position shifts. Nevertheless, this normalization procedure is the chief source of systematic error, resulting in an average variation in $I_{0°}/I_{90°}$ of 16%.

Figure 3 shows the polarizations generated from the measured integrated intensities $I_{0°}$ and $I_{90°}$ taken at polarization angles $\theta=0°$ and 90°, respectively, for the emission peaks A ($2b_1\rightarrow 1a_1$), B ($5a_1\rightarrow 1a_1$), and C ($2b_2\rightarrow 1a_1$) as a function of the incident-beam energy relative

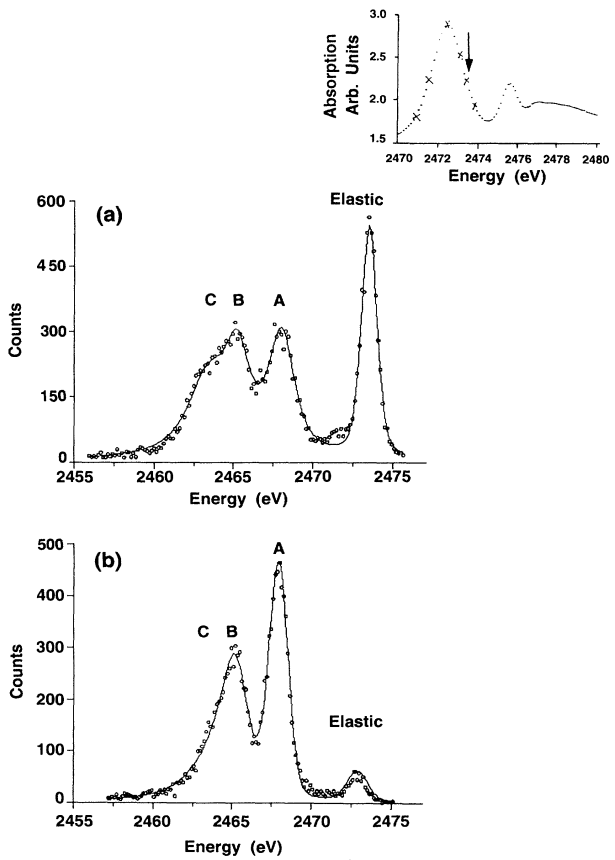

FIG. 2. Identical to Fig. 1 except the excitation energy is at the high-energy side of the subthreshold resonance as denoted by the arrow in the inset.

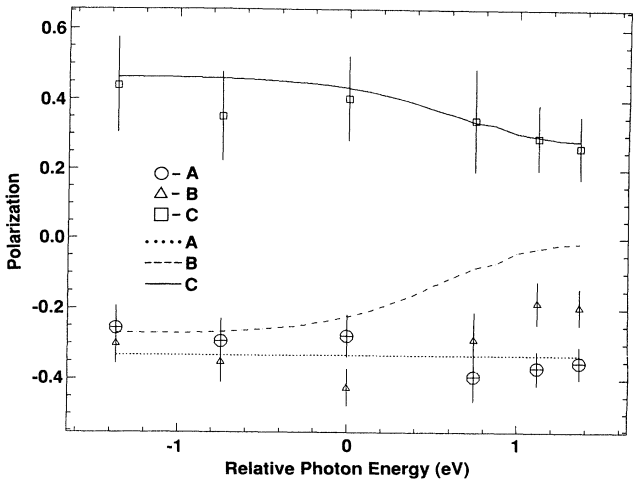

FIG. 3. Polarizations of emission peaks A, B, and C (denoted by ○, △, and □, respectively) as a function of primary beam energy. The lines show predicted polarizations [using Eqs. (4)–(6)] generated from fit shown in Fig. 4 and as described in text. The energy scale is relative to the measured peak absorption energy.

to the peak of the subthreshold resonance (R) (the selected incident beam energies are denoted by $\times$'s in the insets of Figs. 1 and 2). It should be noted that all the emission peaks have significant nonvanishing polarizations for primary photon energies in this region. Peak C has positive polarization and peaks A and B have negative polarization over the entire energy range spanning the resonance. The error bars are due to systematic errors in the normalization procedure as discussed earlier.

DISCUSSION: POLARIZED FLUORESCENCE

For a classical electric dipole absorber and remitter, the polarization[24,25] P is given by $P=(3\cos^2\gamma-1)/(\cos^2\gamma+3)$, where γ is the average angle between the emission and absorption oscillators, and P reaches limiting values $\frac{1}{2}$ and $-\frac{1}{3}$ for angles 0° and 90°, respectively. The directions of the absorption and emission dipole moments with respect to the molecule-fixed coordinates x, y, and z are obtained using the C_{2v} group character table. Thus the $1a_1\rightarrow 3b_2$ and $1a_1\rightarrow 6a_1$ absorption dipole moments point along the y and z axes, respectively. The emission dipole moments for peaks A ($2b_1\rightarrow 1a_1$), B ($5a_1\rightarrow 1a_1$), and C ($2b_2\rightarrow 1a_1$) point along the x, z, and y axes, respectively. The presence of the spectator electron does not affect the directions of the emission dipole moments in the present case. Consequently, the classical model predicts the polarizations of peaks A, B, and C to be $P_A=-\frac{1}{3}$, $P_B=-\frac{1}{3}$, and $P_C=\frac{1}{2}$ for the $1a_1\rightarrow 3b_2$ transition, while $P_A=-\frac{1}{3}$, $P_B=\frac{1}{2}$, and $P_C=-\frac{1}{3}$ for the $1a_1\rightarrow 6a_1$ excitation. It is seen in Fig. 3 that the polarization measurements made using excitation energies at or below the peak of the absorption resonance are consistent with the assignment $1a_1\rightarrow 3b_2$. However, as the excitation energy is increased to the high-energy side of the absorption maximum, the emission peak polarizations vary in a way that is consistent with the additional presence of the $1a_1\rightarrow 6a_1$ excitation. That is, P_A remains large and negative, P_B becomes less negative, and P_C becomes less positive.

There are three possible explanations for the slight depolarization of emission peaks B and C at higher incident-beam energies. In one scenario, the behavior is consistent with a K-shell electron being promoted to a MO with a different symmetry (a_1 symmetry) relative to the dominant MO (b_2 symmetry) and which makes a contribution to the subthreshold absorption resonance intensity at higher primary beam energies as suggested by earlier calculations.[10] That is, the polarization for peaks B and C should change sign ($-\frac{1}{3}\rightarrow\frac{1}{2}$) and ($\frac{1}{2}\rightarrow-\frac{1}{3}$), respectively, while A maintains its polarization ($-\frac{1}{3}\rightarrow-\frac{1}{3}$) as an electron is promoted to an unoccupied MO with a_1 symmetry. Alternatively, the nearby Rydberg-like absorption peak (2475.5 eV), which is composed of S $K\rightarrow np$ transitions, but is only weakly coupled to the molecular symmetry, could contribute to the depolarization. The large polarization of peak A for energies above the resonance peak in Fig. 3, however, seems to contradict this hypothesis. Although there is no experimental evidence, an intriguing explanation for the small depolarization of peaks B and C might be attributed to vibrational dependent polarization.

To examine these possibilities, the resonance peak in the absorption spectrum was fitted (see Fig. 4) with two Voigt peaks. As further motivation, it should be noted that the resonance peak is anomalously broad (approximately 2 eV), asymmetrical, and has some intensity enhancement at higher energies. The subthreshold resonance is not dominated by instrumental broadening as can be seen from the observation that the Rydberg peak has a width of only approximately 1 eV. In the absence of calculations and polarization measurements, the broad absorption resonance peak might be attributed to vibrational excitation of the molecule during absorption. The numerical fit found a peak separation of 0.69 eV with the higher-energy peak (presumably due to the a_1 unoccupied orbital) having an integrated intensity of only 20% relative to the dominant b_2 contribution. The calculations of Mazalov *et al.*[10] indicate that the molecular orbital with b_2 symmetry lies about 0.5 eV below the one with a_1 symmetry, in good agreement with the results reported here, while Schwarz's[11] calculations indicate the opposite order with an energy separation of 0.7 eV. LaVilla[13] inferred an energy separation of "about 1 eV" with the high-energy component being 15% of the more intense component and without explicitly assigning a symmetry to each of the two unoccupied MO's. A Voigt function also was used to fit the Rydberg peak. At the primary energy (see Fig. 2) where the polarization of emission peaks B and C diminish (2473.6 eV), the small-component contribution (from the fit) to the resonance peak dominates (by a factor of 6) over the contribution from the Rydberg peak.

The fitted results to a two-component absorption resonance shown in Fig. 4 may be used with the corresponding classical-model predictions of polarization to model

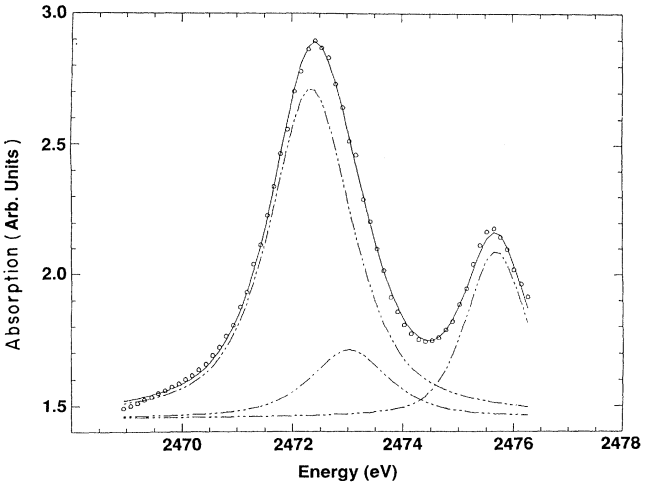

FIG. 4. Solid curve is calculated using two Voigt peaks (from the best fit, energy separation 0.69 eV, relative peak height ratio approximately 5:1) for subthreshold resonance peak in H_2S absorption spectrum plus a third peak for the lowest-energy Rydberg peak.

the observed polarizations displayed in Fig. 3. The polarization predicted for an unresolved combination of transitions is obtained by making use of the polarization anisotropy R,[26–28] defined by

$$R=\frac{I_{0^\circ}-I_{90^\circ}}{I_{0^\circ}+2I_{90^\circ}}\ , \tag{2}$$

which can be related to the polarization P by

$$P=\frac{3R}{2+R}\ . \tag{3}$$

The R value for unresolved transitions is given by an average of the classical-model values weighted by energy-dependent relative intensities $I(3b_2)$ and $I(6a_1)$ determined from the numerical fits shown in Fig. 4. The predicted individual energy-dependent R values for each of the x-ray emission peaks in Figs. 1 and 2 are given by

$$R_A=-\tfrac{1}{5}\ , \tag{4}$$

$$R_B=-\frac{1}{5}\frac{I(3b_2)}{I(3b_2)+I(6a_1)}+\frac{2}{5}\frac{I(6a_1)}{I(3b_2)+I(6a_1)}\ , \tag{5}$$

$$R_C=\frac{2}{5}\frac{I(3b_2)}{I(3b_2)+I(6a_1)}-\frac{1}{5}\frac{I(6a_1)}{I(3b_2)+I(6a_1)}\ . \tag{6}$$

The corresponding polarizations for each of the x-ray emission peaks can then be derived by using Eq. (3). The polarizations predicted using this model along with the experimental results are shown in Fig. 3.

The model curves in Fig. 3 are qualitatively consistent with the experimental data giving credence to the two-component model. The model, however, overestimates the effect of the weaker $(6a_1)$ component on the emission polarization for peak B. These differences between the predictions and experimental results may be due to systematic errors and theoretical uncertainties. The relative intensities of the two components derived from deconvolution of the observed absorption spectrum may be inaccurate due to the inability to resolve its structure. Although the absorption spectrum is primarily lifetime broadened, a comparison with previous results[13] indicates that there is an instrumental contribution to the peak widths. Hence a better resolved absorption spectrum could be obtained and used to find better values for $I(6a_1)$ and $I(3b_2)$. Using a Si(111) monochromator instead of the Ge(111) monochromator would have improved the energy resolution of the absorption spectrum at the cost of incident flux.

It should be noted that the model relies on classical values for the polarization. The classical model is valid for rotational angular momentum $J\sim\infty$, but at room temperature (using a principle axis with the largest moment of inertia) $J\sim 6$ for H_2S leading to small corrections (15%) in the predicted classical values. In the model describing the unresolved resonance, it is also assumed that the radiative yields for the two absorption resonances are the same and are unaffected by the presence of spectator electrons. Theoretical studies of the relative intensities and radiative yields of the two absorption resonances would be useful to help resolve these issues.

The depolarization of the emission peaks therefore cannot be attributed to contributions from the Rydberg peak in the absorption spectrum. More likely, as the energy is increased, the incident beam excites nearly degenerate orthogonal MO's and the observed polarization is the result of partial cancellation of the polarizations from a superposition of emission spectra. To summarize, this hypothesis is supported by the XES polarization and its dependence on primary photon energy, the absorption spectrum, and previous calculations.

RESULTS: MULTIVACANCY SATELLITES

As the energy of the incident beam is raised to an energy about 5.7 eV above the S 1s threshold, a shoulder (labeled A') develops on the high-energy side of the emission peak A (see inset of Fig. 5). The absence of a high-energy shoulder in the emission spectra of Figs. 1(a), 1(b), 2(a), and 2(b) for subthreshold excitation energy should be noted. As shown in Fig. 5, the ratio of the integrated intensity of the shoulder (A') to the integrated intensity of the total K-V emission spectrum (excluding the shoulder A') as a function of incident beam energy indicates an energy onset, slowly increases, and eventually approaches an asymptotic value. The K-shell binding energy (2478.3 eV) is labeled as S K^{-1} in Fig. 5. Figure 5 also shows the approximate additional energy (not accounting for screening effects and relaxation) to promote an electron from the highest occupied molecular orbital (HOMO) (it is not certain which MO is excited, so this is a very rough value) to the lowest-energy unoccupied molecular orbital [(LUMO) or the subthreshold absorption resonance] and is labeled as Sats (2478.3 + 4.5 eV).

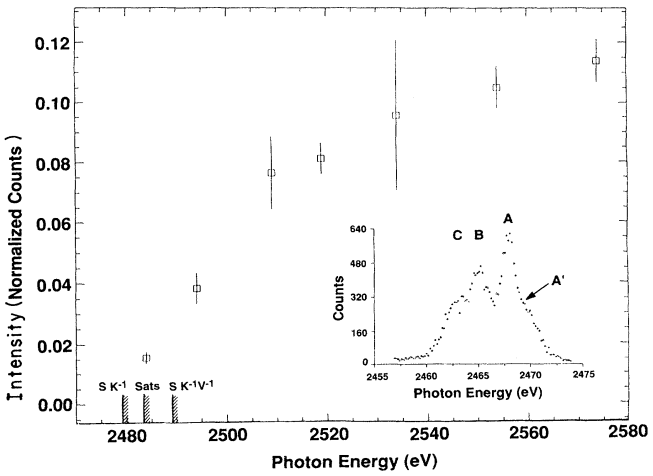

FIG. 5. Ratio of satellite or shoulder (peak a') integrated intensity to the integrated intensity of the K-V spectrum. Also indicated are the K-electron binding energy S K^{-1}, S K^{-1} plus the LUMO-HOMO energy (as discussed in the text) labeled Sats, and the double-ionization energy labeled S $K^{-1}V^{-1}$, which equals S K^{-1} plus the HOMO binding energy. The inset shows the high-energy satellite peak A' which is absent in Fig. 1, generated by an incident beam with energy of 2530 eV, or 60 eV above threshold.

The marker labeled with $K^{-1}V^{-1}$, the double-ionization threshold energy, indicates the approximate additional energy to ionize an electron from the HOMO (2478.3+10.5 eV), again without accounting for screening and relaxation. This estimate for the double-vacancy threshold also does not consider the enhanced charge of the core due to double ionization and therefore the threshold energy is expected to be larger. The relative intensity of the emission satellite A' (Fig. 5) as a function of incident-beam energy suggests that initially the satellite can be attributed to K-hole formation and electron excitation to an unoccupied valence orbital. At higher energies, double ionization as in argon[4] and suggested by LaVilla[13] also may contribute to the satellite intensity. The onset at high primary photon energy and the gradual increase in intensity with increasing excitation energy are inconsistent with contamination as suggested by Mazalov *et al.*[12]

RESULTS: INNER VALENCE

Finally, photoelectron spectra[29–31] indicate the presence of additional emission spectral features originating from a more tightly bound orbital (approximately 12 eV with respect to the A emission peak) corresponding to $4a_1 \rightarrow 1a_1$. Calculations[14] predict the relative x-ray emission intensity for this feature to be 0.03 of the largest emission peak A after accounting for the broader widths. The low intensity is due to the small S $3p$ contribution to the tightly bound MO,[30–32] which is primarily of S $3s$ character. Following examination in the appropriate energy region in the emission spectra,[20–22] no discernible peaks were observed above background indicating the peak intensity is less than 1% of the large peak A intensity.

SUMMARY

In summary, the x-ray emission spectrum of the molecule H_2S is strongly polarized following excitation of a sulfur K-shell electron to a subthreshold resonance with a polarized x-ray beam. The polarization of the emission spectrum as the incident beam's energy is scanned across the resonance reveals that the resonance is mostly due to an unoccupied orbital of $3b_2$ symmetry while some contribution from the $6a_1$ symmetry orbital appears at an energy slightly above the peak in the subthreshold absorption. The experimentally observed polarization behavior of the emission spectrum is in closer agreement with the calculations for the absorption spectrum of Mazalov *et al.*[10] rather than Schwarz.[11] An extra feature appears at the high-energy end of the emission spectrum only for excitation energies exceeding the K-shell electron ionization threshold and is attributed to multiple-vacancy formation and not to contamination of the sample cell. Emission from the inner-valence orbital $4a_1$ was below the detection limit of 1% and the calculated value of 3%.

ACKNOWLEDGMENTS

We thank B. A. Karlin for technical assistance in performing these measurements. This research was carried out (in part) at the National Synchrotron Light Source, Brookhaven National Laboratory, which is supported by the U.S. Department of Energy, Division of Materials Sciences and Division of Chemical Sciences.

[1]A. Meisel, G. Leonhardt, and R. Szargan, *X-Ray Spectra and Chemical Binding* (Springer-Verlag, Berlin, 1989).
[2]V. N. Nefedov, J. Struct. Chem. **13**, 334 (1972).
[3]R. C. C. Perera, P. L. Cowan, D. W. Lindle, R. E. LaVilla, T. Jach, and R. D. Deslattes (unpublished).
[4]R. D. Deslattes, R. E. LaVilla, P. L. Cowan, and A. Henins, Phys. Rev. A **27**, 923 (1983).
[5]F. Kh. Gelmukhanov and L. N. Mazalov, Opt. Spectrosc. **42**, 371 (1977).
[6]D. W. Lindle, P. L. Cowan, R. E. LaVilla, T. Jach, R. D. Deslattes, B. Karlin, J. A. Sheehy, T. J. Gil, and P. W. Langhoff, Phys. Rev. Lett. **60**, 1010 (1988).
[7]U. Fano and J. H. Macek, Rev. Mod. Phys. **45**, 553 (1973).
[8]C. H. Greene and R. N. Zare, Annu. Rev. Phys. Chem. **33**, 119 (1982).
[9]S. Bodeur and J. M. Esteva, Chem. Phys. **100**, 415 (1985).
[10]L. N. Mazalov, A. P. Sadovskii, P. I. Vadash, and F. G. Gel'mukhanov, J. Struct. Chem. **14**, 234 (1973).
[11]W. H. E. Schwarz, Chem. Phys. **11**, 217 (1975).
[12]L. N. Mazalov, A. P. Sadovskii, V. M. Bertenev, V. V. Murakhtanov, E. A. Gal'tsova, and L. I. Chernyaski, Theor. Exp. Chem. **7**, 37 (1971).
[13]R. E. LaVilla, J. Chem. Phys. **62**, 2209 (1975).
[14]S. Polezzo, M. P. Stabilini, and M. Simonetta, Mol. Phys. **17**, 609 (1969).
[15]P. L. Cowan, S. Brennan, R. D. Deslattes, A. Henins, T. Jach, and E. G. Kessler, Nucl. Instrum. Methods A **246**, 154 (1986); P. L. Cowan, S. Brennan, T. Jach, D. W. Lindle, and B. A. Karlin, Rev. Sci. Instrum. **60**, 1603 (1989).
[16]P. L. Cowan, J. B. Hastings, T. Jach, and J. P. Kirkland, Nucl. Instrum. Methods **208**, 349 (1983).
[17]A. Henins, E. G. Kessler, and P. L. Cowan, Nucl. Instrum. Methods **208**, 287 (1983).
[18]S. Brennan, P. L. Cowan, R. D. Deslattes, A. Henins, D. W. Lindle, and B. A. Karlin, Rev. Sci. Instrum. **60**, 2243 (1989).
[19]G. G. Luther, P. L. Cowan, A. Henins, and S. Brennan, Nucl. Instrum. Methods A **246**, 537 (1986)
[20]A. W. Potts and W. C. Price, Proc. R. Soc. London Ser. A **326**, 181 (1972).
[21]M. Y. Adam, P. Morin, C. Cauletti, and M. N. Piancastelli, J. Electron Spectrosc. **36**, 377 (1985).
[22]C. E. Brion, Y. Iida, and J. D. Thomson, Chem. Phys. **101**, 449 (1986).
[23]D. W. Lindle, P. L. Cowan, T. Jach, R. E. LaVilla, R. D. Deslattes, and R. C. C. Perera, Phys. Rev. A (to be published).
[24]M. McClintock, W. Demtroder, and R. N. Zare, J. Chem. Phys. **51**, 5509 (1969).
[25]M. Macpherson, J. P. Simons, and R. N. Zare, Mol. Phys. **38**, 2049 (1979).

[26]E. D. Poliakoff, J. L. Dehmer, D. Dill, A. C. Parr, K. H. Jackson, and R. N. Zare, Phys. Rev. Lett. **46**, 907 (1981).
[27]J. A. Guest, K. H. Jackson, and R. N. Zare, Phys. Rev. A **28**, 2217 (1983).
[28]R. N. Zare, *Angular Momentum* (Wiley, New York, 1988).
[29]M. Y. Adam, C. Cauletti, and M. N. Piancastelli, J. Electron Spectrosc. **42**, 1 (1987).
[30]H. Wasada and K. Hirao, Chem. Phys. **138**, 277 (1989).
[31]W. Domcke, L. S. Cederbaum, J. Schirmer, W. von Niesson, and J. P. Maier, J. Electron Spectrosc. **14**, 59 (1978).
[32]C. L. French, C. E. Brion, and E. R. Davidson, Chem. Phys. **122**, 247 (1988).